Molecular Cell, Volume *51*

Supplemental Information

Tandem Stem Loops in roX RNAs Act Together to Mediate X- Chromosome Dosage Compensation in *Drosophila*

Ibrahim Avsar Ilik, Jeffrey J. Quinn, Plamen Georgiev, Filipe Tavares-Cadete, Daniel Maticzka, Sarah Toscano, Yue Wan, Robert C. Spitale, Nicholas Luscombe, Rolf Backofen, Howard Y. Chang, and Asifa Akhtar

Supplemental Information Inventory

Figure S1, related to Figure 1. This figure shows the biochemical characterization of MLE.

Figure S2, related to Figure 2. This figure summarizes iCLIP results and gives a rationale for barcode error compensation.

Figure S3, related to Figure 2. This figure shows the reproducibility of MLE and MSL2 iCLIP data among biological replicates for roX1, roX2, rRNA CR41602, ko and CG13654 genes.

Figure S4, related to Figure 3. This figure complements Figure 3 by providing all the structural data on the 3'-end of roX1 RNA.

Figure S5, related to Figure 3. This figure complements Figure 3 by providing all the structural data on the full-length roX2 RNA.

Figure S6, related to Figures 5 and 6. This figure shows the result of a HITS-CLIP experiment in S2 cells, indicating that MLE protein protects the helical structures at the 5'-end of roX2 exon-3. It also shows additional EMSA experiments that show the interaction between MLE's N-terminus and 5'-end of roX2 exon-3.

Figure S7, related to Figure 7. It shows the effects of using a weaker GAL4 driver on male viability. It also contains supporting data for GRNA experiments presented in Figure 6.

Supplementary Figure 1

A

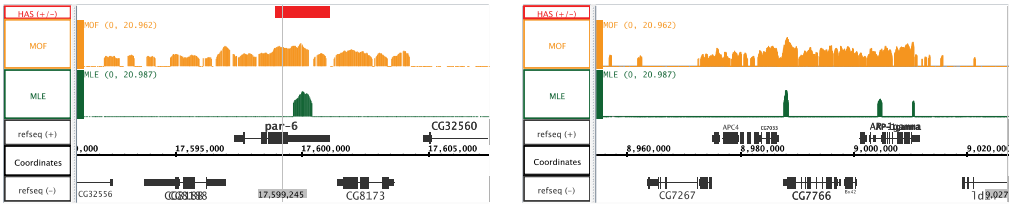

B

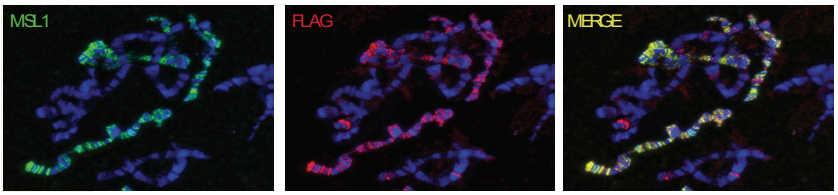

C

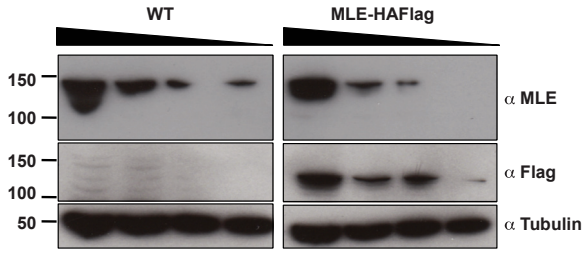

D

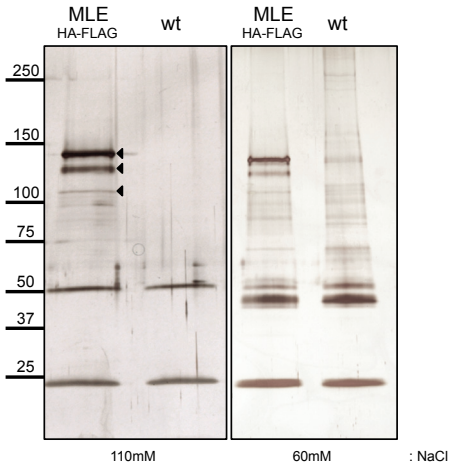

E

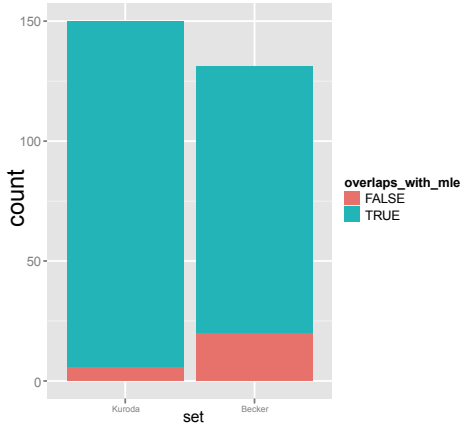

Figure S1.

Biochemical analysis of MLE.

MLE ChIP-seq analysis. **(A)** MLE (green) binds to HAS regions (left) as well as low affinity sites (LAS) (right), but in a weaker and more restricted fashion compared to MOF (orange). A browser snapshot for par6 HAS (left) and a snapshot for a LAS (right) is shown for MLE and MOF binding. **(B)** An MLE transgene, tagged with HA and FLAG at its C-terminus rescues male lethality in an mle-null background, restores MSL1 staining on the X-chromosome and localizes to the X-chromosome like the wild-type protein. Polytene chromosomal staining using antibodies against endogenous MSL1 (green) and Flag tagged MLE (red) show perfect co-localization (merge, yellow). **(C)** Western blot analysis of extracts prepared from embryos carrying the MLE-HA-FLAG transgene show that the MLE transgene is not over-expressed compared to the endogenous MLE protein. Tubulin is used as a control. **(D)** Tandem affinity purification of MLE from nuclear extracts prepared from mle^{1}; MLE-HA-FLAG flies does not result in the co-purification of the MSL-complex or any other protein. Arrowheads show the bait, MLE-HA-FLAG. Decreasing the salt (NaCl) concentration from 110mM to 60mM during the purification procedure increases background but not the quality of the purification. **(E)** MLE ChIP-seq analysis shows a great degree of overlap between MLE binding sites and the previously identified High-Affinity Sites (HAS) on the X-chromosome. Related to Figure 1.

Supplementary Figure 2

A

MLE iCLIP	Replicate 1	Replicate 2	Replicate 3	Total
Reads	49,744,886	8,976,213	34,460,608	93,181,707
Mapped read pairs	40,668,737	7,531,060	27,668,364	75,868,161
Uniquely aligned read pairs	24,954,209	3,800,546	17,743,605	46,498,360
Cross-link events after PCR duplicate removal	301,610	38,697	454,046	794,353
Cross-link events after barcode error compensation	37,117	6,123	49,185	92,425
Cross-link events after shuffling	15,643	1,764	29,468	46,875
Cross-link nucleotides	963	179	1,705	2,847

MSL2 iCLIP	Replicate 1	Replicate 2	Replicate 3	Total
Reads	37,745,073	51,701,140	1,290,584	90,736,797
Mapped read pairs	28,637,172	36,580,377	1,237,893	66,455,442
Uniquely aligned read pairs	15,872,442	21,789,940	27,038	37,689,420
Cross-link events after PCR duplicate removal	776,539	652,759	4,068	1,433,366
Cross-link events after barcode error compensation	178,505	213,290	3,478	395,273
Cross-link events after shuffling	55,176	65,718	49	120,943
Cross-link nucleotides	3,205	2,928	14	6,147

B

random barcode	#reads	class	frac_top
TATTG	448	top	1
TGTTG	6	1MM	0.013
CATTG	3	1MM	0.007
AATTG	2	1MM	0.004
TTTTG	2	1MM	0.004
GATTG	1	1MM	0.002
TATAG	1	1MM	0.002

C

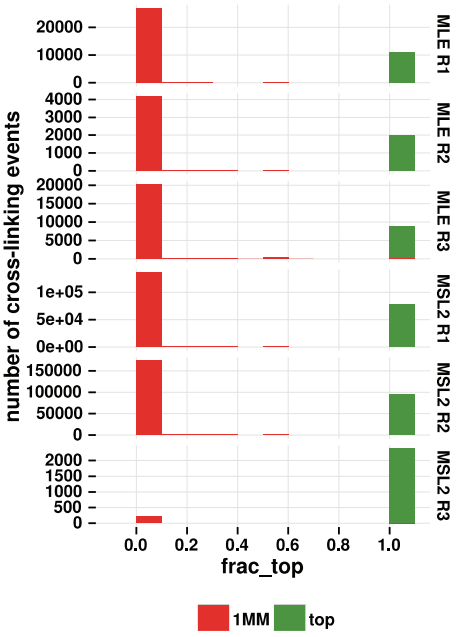

D

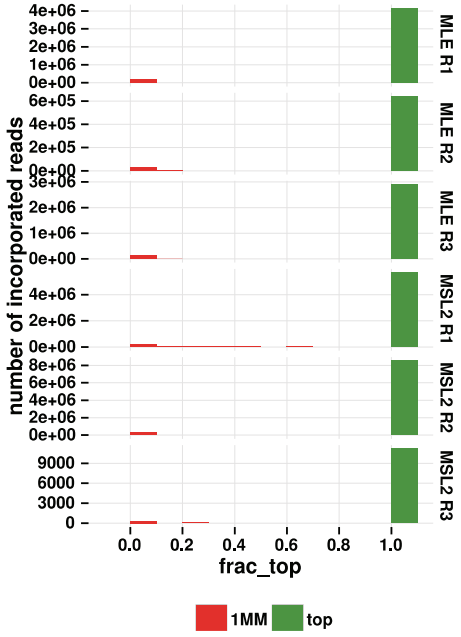

E

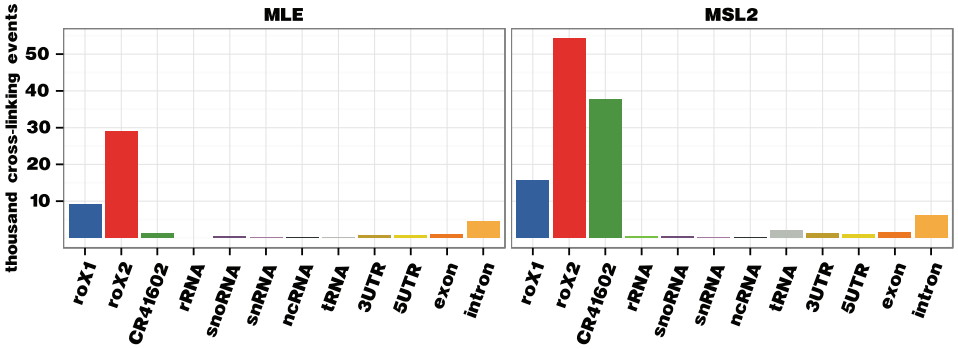

Figure S2.

iCLIP analysis details.

(A) iCLIP pipeline statistics. **(B)** Errors introduced into random barcodes during library preparation or sequencing can cause spurious cross-linking events when cross-linking events are represented by many PCR duplicates. As a typical example, we show the cross-linking events for MLE replicate 1 position 243,144 on chromosome 2L. At this position, 463 paired-end reads were combined into 7 cross-linking events. The majority of these reads were assigned to a single cross-linking event with barcode TATTG. The remaining 6 cross-linking events incorporate only 3% of the read pairs assigned to this position and each barcode only differs in a single nucleotide to the barcode of the 'top' event. Assuming 3% of random barcodes contain a single error, all but the 'top' event in this example must be categorized as false event and should be removed. This error rate matches the error rate seen for the replicate barcodes: 5% of the MLE replicate barcodes and 4% of the MSL2 replicate barcodes had single nucleotide errors. **(C)** Without compensating for errors in random barcodes, the majority of cross-linking events are false events. From each set of cross-linking events on the autosomes having the same end coordinates (as used for removal of PCR duplicates), we selected the event incorporating the largest number of read pairs (top) and all events with exactly one mismatch in the random barcode as compared to the random barcode of the 'top' event (1MM). For each cross-linking event we calculated the fraction of incorporated reads with respect to the number of reads of the corresponding top event (frac_top). The histogram shows that there are many more 1MM events than top events. Most of these events, however, incorporate less than 10% reads as compared to the corresponding top events and should thus be considered false events. For all replicates (except MSL2 replicate 3 which was removed from further analysis), the number of false 1MM events is higher than the number of corresponding top events. **(D)** Albeit the shear number of 1MM events is high, the associated number of reads is low. Similar to previous figure, but counting the number of incorporated reads instead of the number of cross-linking events. False cross-linking events are supported by a tiny fraction of all reads, showing that removal of spurious cross-linking events will retain most of the available reads. **(E)** Distribution of cross-

linking events. Each cross-linking event was assigned the first matching target class following the hierarchy roX1, roX2, CR41602, rRNA, snoRNA, snRNA, ncRNA, tRNA, 3UTR, 5UTR, exon, intron. Related to Figure 2.

Supplementary Figure 3

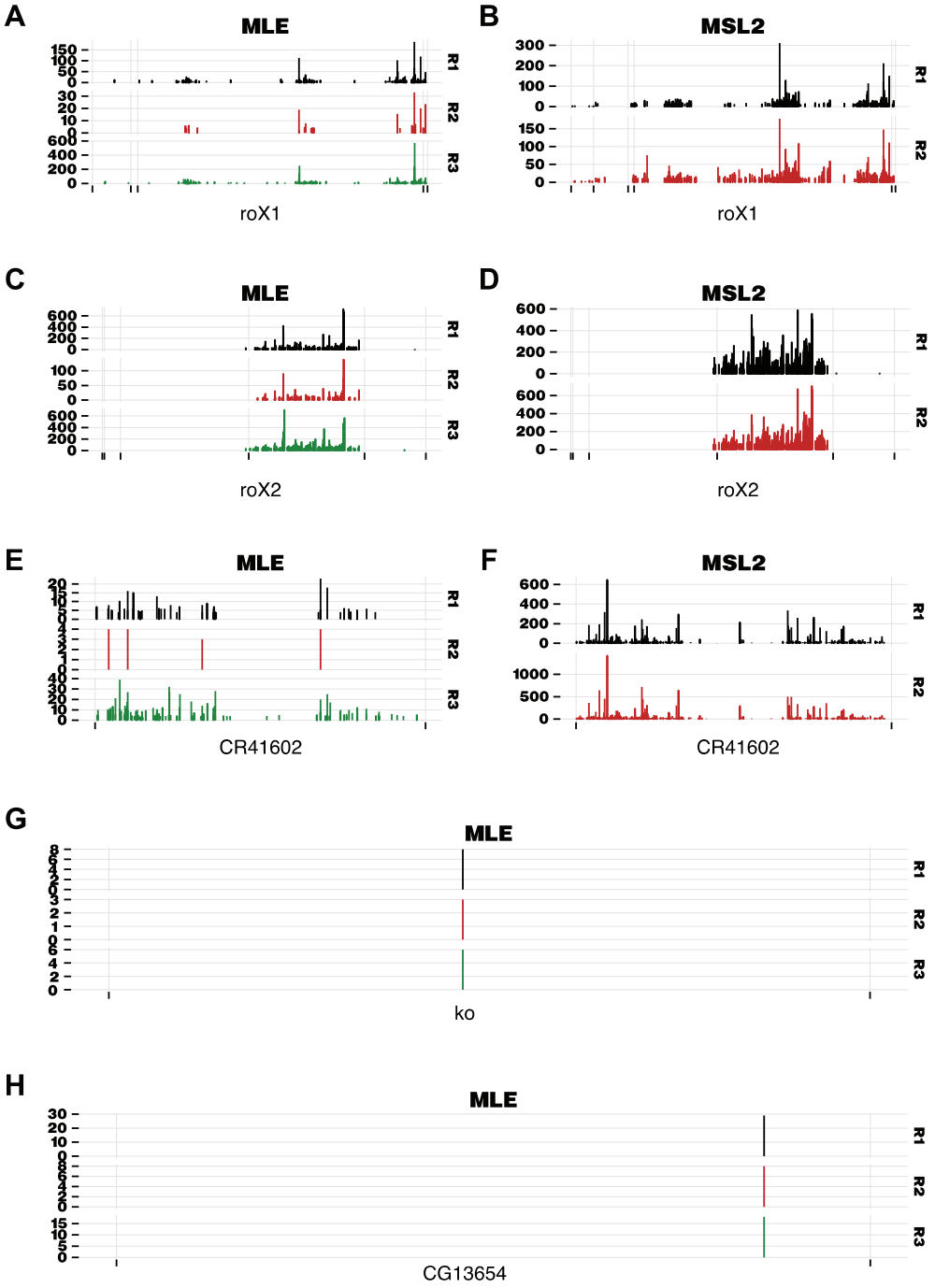

Figure S3.

Reproducibility of iCLIP data.

Nucleotides scored by number of cross-linking events for MLE and MSL2 on roX1 **(A-B)**, roX2 **(C-D)** and rRNA CR41602 **(E-F)**. The profiles show good agreement between replicates. **(G-H)** Two examples of MLE binding ko and CG13654. In contrast to the previous profiles, binding to ko and CG13654 is restricted to a single nucleotide. Related to Figure 2.

Supplementary Figure 4

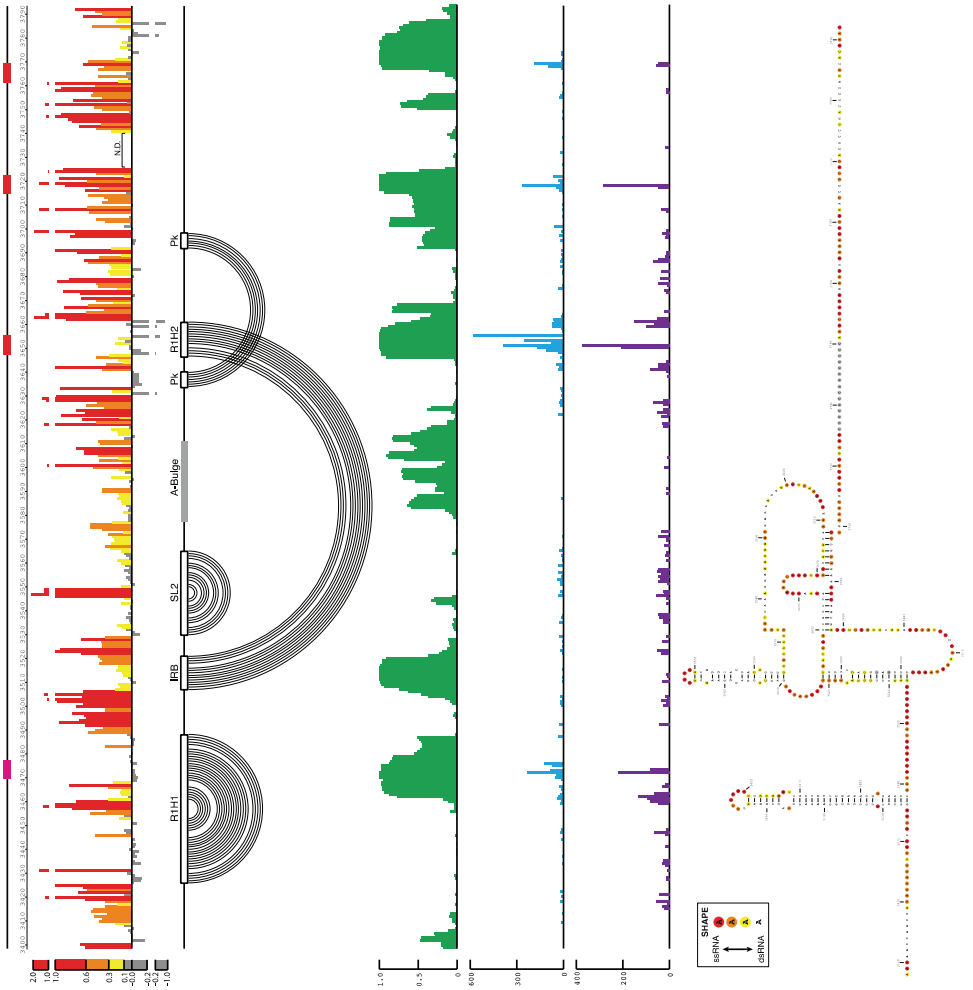

Figure S4.

The structure of the 3'-terminus of roX1.

(A-B) We interrogated the structure of the 3'-terminus of roX1 by SHAPE. Due to spurious reverse transcriptase stops, the reactivities of bases 3656, 3658, and 3726-3740 could not be measured (N.D.). We provide evidence for the existence of the stem-loop proposed by Stuckenholz and colleagues (Stuckenholz et al., 2003) (SL1), which we call the roX1 helix1 (R1H1). We also find evidence of Kelley's (Kelley et al., 2008) proposed long-range interaction between the inverse roX box (IRB) and roX box-1 (RB1), as well as "stem-loop 2" (which we refer to as P2), a stem-loop in the loop of the IRB/RB1 helix. We also find evidence for a pseudoknot (Pk) between the loop of IRB/RB1 and a region immediately 5' of roX box2. RB2 and RB3 are not double-stranded. The A-bulge (an A-rich, low complexity region) has low reactivity and likely base-pairs with one or more of the U-rich low complexity regions of roX1. **(C)** The RBs of roX1 are highly conserved, as well as the IRB. Most of the RNA is poorly conserved. **(D-E)** MLE iCLIP peaks fall on or near roX boxes, whereas MSL2 iCLIP peaks are more diffuse along roX1. **(F)** Structure model for the 3'-terminus of roX1 with SHAPE reactivity annotations. Related to Figure 3.

Supplementary Figure 5

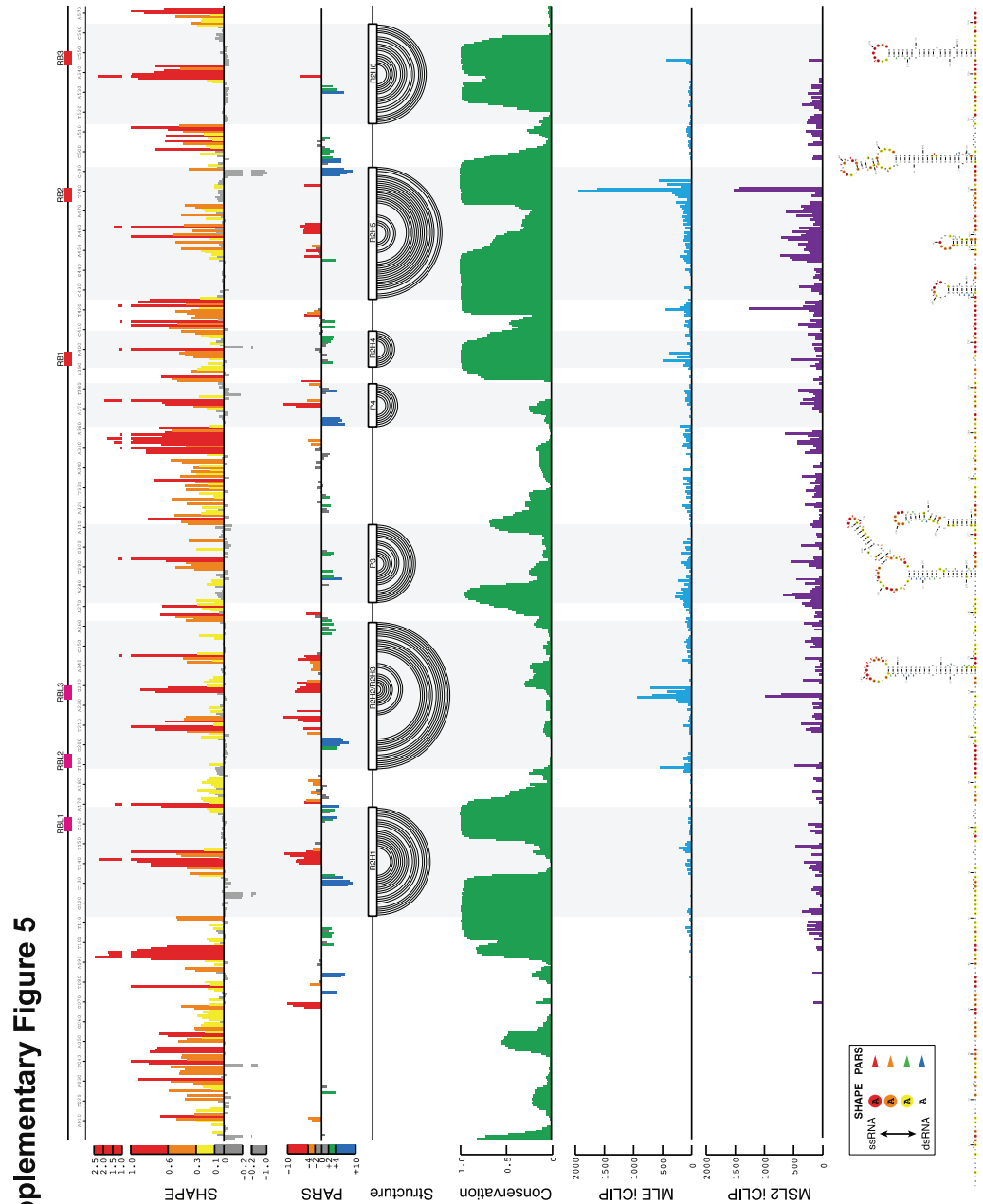

Figure S5.

The global structure of roX2.

(A) We interrogated the flexibility of each base in the major spliced isoform of roX2 (573nt) using SHAPE. Flexible, unpaired bases have high reactivity scores, whereas paired bases have low reactivity scores. **(B)** To complement the SHAPE data, we also performed enzymatic digestion of roX2 with structure-specific ribonucleases (RNases), then sequenced the RNA fragments (following PARS(Kertesz et al., 2010)). The PARS score of each base is calculated as LOG2[(V1 reads + 1)/(S1 reads + 1)] and the data is filtered to include the top 20% covered bases so as to eliminate noise from poor sequencing coverage. Bases that are cleaved more by V1 RNase have a positive PARS score and are double-stranded (blue and green), whereas bases that are cleaved more by S1 RNase have a negative PARS score and are single-stranded (red and orange). Note that the y-axis is inverted so as to correlate with SHAPE data. **(C)** The structure of roX2 is represented in circle plot notation, indicating base-pairing partners. Stable local secondary structures are shown by loops and highlighted in gray. **(D)** Conservation score between 12 *Drosophila* species and 3 non-*Drosophila* insects. Note the high conservation of roX boxes and their associated helix stems. **(E)** MLE iCLIP peaks correspond to double-stranded regions of roX2 on or near roX boxes. **(F)** MSL2 iCLIP peaks are more diffuse along roX2. **(G)** The global structure of roX2 annotated with SHAPE and PARS scores (filled circles and arrowheads, respectively). Related to Figure 3.

Supplementary Figure 6

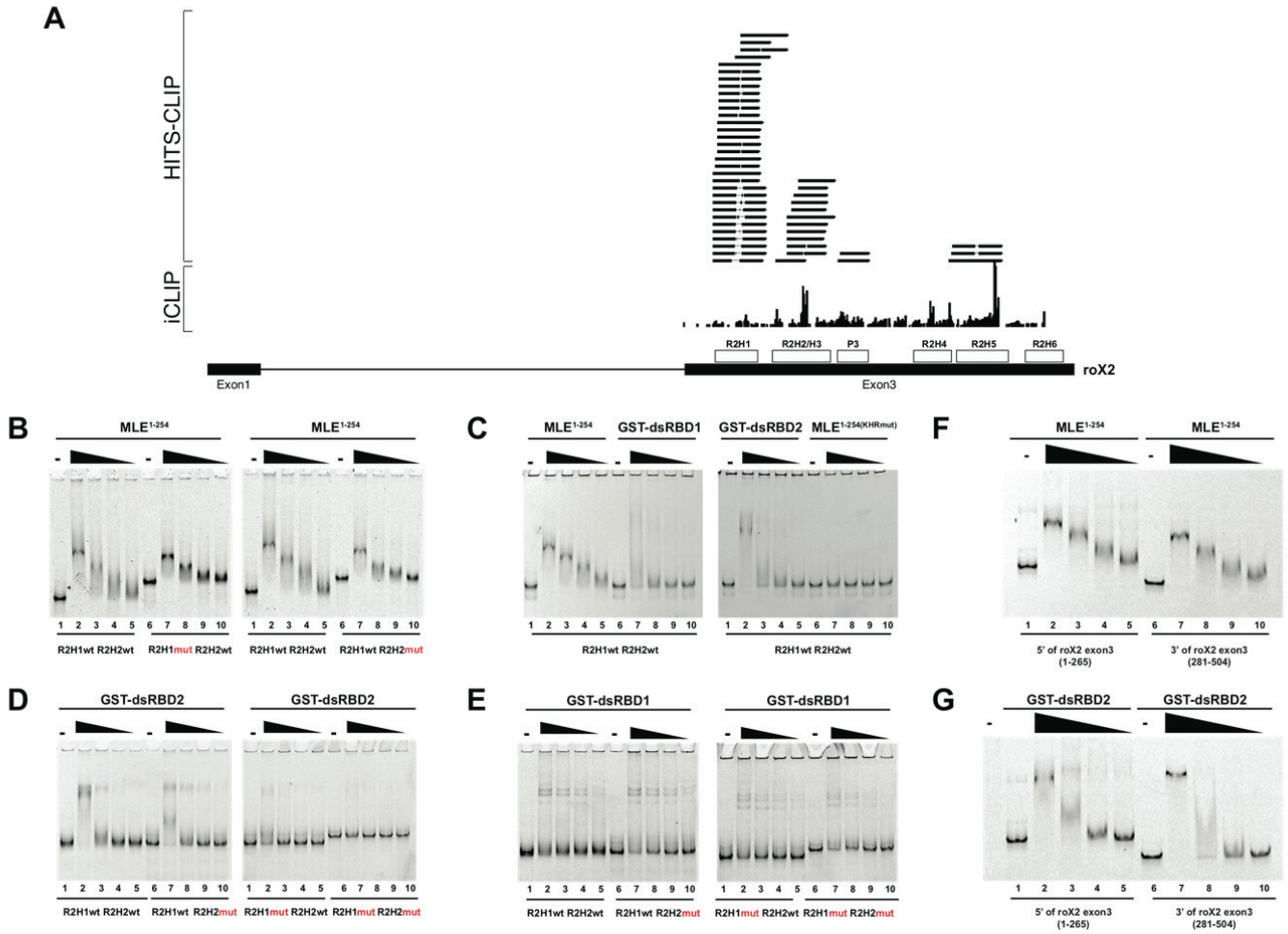

Figure S6.

HITS-CLIP and gel shift analysis of MLE.

(A) HITS-CLIP shows preferential binding of MLE to the 5'-end of roX2 exon3. As opposed to iCLIP, HITS-CLIP protocol requires the reverse-transcriptase to run through the cross-linked residue(s), and thus can result in different binding profiles on a given RNA, especially if the protein of interest contains multiple (ds)RNA interacting domains. We show here that both methods agree on the regions of roX2 that MLE interacts with, but differ in the details. The HITS-CLIP data show that MLE interacts mostly with R2H1 followed by R2H2/3 and P3; we also detect a small but significant binding at R2H5. Interestingly, although the iCLIP data also show that R2H1 and R2H2/3 are among the best MLE targets, R2H5 stands-out as the most significantly bound structure in the RNA (Figure 5B). We currently do not know if the binding of different domains to RNA can result in different types of cross-links that may lead to more efficient reverse-transcriptase termination than other types of cross-links, which can lead to higher scores of binding in iCLIP. Finally, the gaps that appear in the middle of some HITS-CLIP reads that map to R2H1 fall exactly on the loop region of this stem-loop, which is an evidence for the existence of these structures *in vivo*. CLIP-tags are shown as black boxes. iCLIP track shown here indicates only the most prominent peaks. Schematic representation of roX2 RNA and conserved domains in exon-3 is indicated at the bottom. **(B-G)** The N-terminal dsRBDs of MLE show preferential binding to different stem-loops of roX2 exon3. **(B)** The first 254 amino acids of MLE (MLE^{1-254}) that contains the two dsRBDs in tandem (dsRBD1+2) interact with a roX RNA probe consisting of R1H1 and R2H2/3 (R2H2) (Lanes 2-5). Mutating either R2H1 (lanes 7-10, left) or R2H2 (lanes 7-10, right) slightly reduces this interaction, showing that the presence of either structure is sufficient for the MLE interaction with roX2. Corresponding mutations are indicated in red. **(C)** MLE^{1-254} (dsRBD1+2 wt, lanes 2-5, left), and the single dsRBD domains (GST-dsRBD1 lanes 7-10, left and GST-dsRBD2 lanes 2-5, right) interact with a roX RNA probe consisting of R1H1 and R2H2/3 (R2H1wtR2H2wt) *in vitro*. A triple mutant form of MLE dsRBD1+2 (K4E H196E R198E) (lanes 7-10, right) no longer interacts with this probe. **(D)** MLE dsRBD2 preferentially interacts with R2H1 in roX2 RNA. Mutations in R2H2 (compare

lanes 7-10, left with lanes 2-5, left) had little effect on RNA interaction. However, mutating R2H1 (compare lanes 2-5, right with lanes 2-5, left) led to significant reduction in RNA binding whereas mutating both helices abolished this interaction (lanes 7-10, right). These observations suggest that MLE dsRBD2 preferentially interacts with R2H1. **(E)** Same as in **(D)** but this time using GST-dsRBD1**.** Mutating R2H1 (compare lanes 2-5, right with lanes 2-5, left) does not appreciably affect the interaction between GST-dsRBD1 and the RNA probe. Similarly mutating neither R2H2 (lanes 7-10, right with lanes 2-5, left) nor mutating both helices (lanes 7-10, right) does not seem to affect this interaction suggesting that it is not specific to double-stranded RNA. **(F)** MLE^{1-254} (dsRBD1+2) interacts with the 5'-end (1-265, lanes 2-5) and the 3'-end of roX2 exon3 (281-504, lanes 7-10) with the apparent affinity. **(G)** Same as in **(F)** but this time using GST-RBD2. Similar to MLE^{1-254} (dsRBD1+2), GST-dsRBD2 interacts both with the 5'-end (1-265, lanes 2-5) and the 3'-end of roX2 exon3 (281-504, lanes 7-10), unlike dsRBD1+2, GST-dsRBD2 seems to interact more efficiently with the 5'-end of roX2 as compared to the 3'-end. For each protein derivative 125nM, 250nM, 500nM, 1μM respectively was titrated (black triangle). In all gels free RNA probe is shown in lanes 1 and 6. Mutated RNA helices are indicated in red. Related to Figures 5 and 6.

Supplementary Figure 7

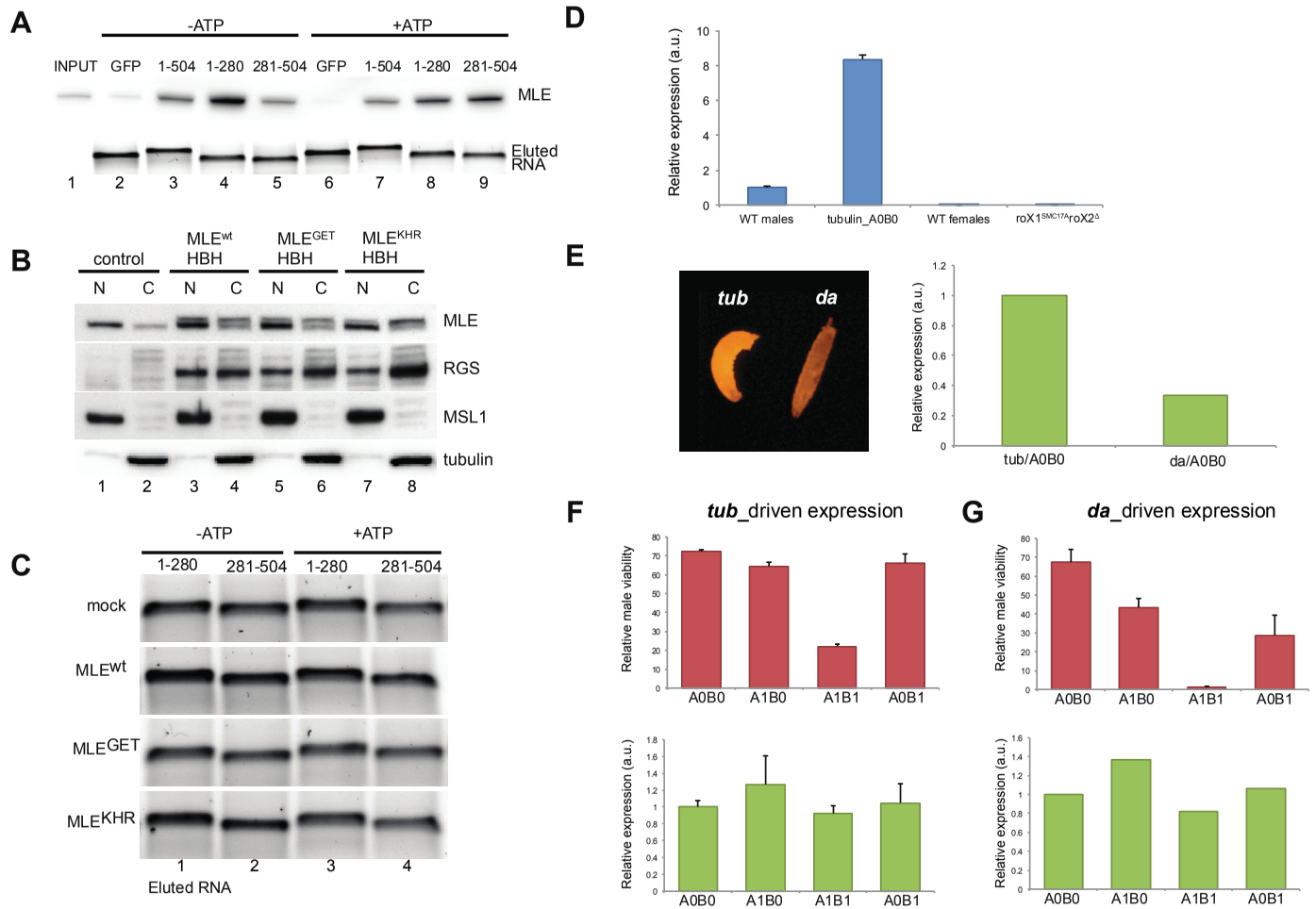

Figure S7.

In vitro and in vivo characterization of MLE-roX2 interaction.

(A) GRNA chromatography in the absence of ATP shows that MLE interacts preferentially with the 5'-end of roX2 (1-280, lane 4). Adding ATP into the very same reactions (lanes 6-9) leads to a reduction of MLE's interaction with the full-length roX2 exon-3 (compare lanes 3 and 7) but also with the GFP RNA which serves as a measure of background binding. Interestingly, the interaction between MLE and the 3'-end of roX2 (281-504, lanes 5 and 9) is enhanced upon addition of ATP. Eluted RNA (bottom) indicates the RNA left on the beads at the end of the experiment and assures that observed changes in MLE binding is not the result of differential RNA loading. RNAs were loaded on 1% agarose gels and revealed by SYBR Safe staining. **(B)** Nuclear (N)-cytoplasmic (C) extracts prepared from S2 cells either mock transfected (Control, lanes 1-2) or transfected with different MLE constructs (indicated on top, lanes 3-8) show that endogenously expressed MLE, together with the wild-type (MLE^{wt}) and mutant MLE constructs (MLE^{GET}, MLE^{KHR}) tagged with the HBH epitope can be found both in the nucleus and the cytoplasm, although with different ratios. Antibodies used for immunoblotting are showed on the right. RGS is an epitope that is specific to the transgenic MLE constructs. **(C)** Eluted RNA levels indicate that observed differences in transgenic and endogenous MLE binding to the 5'- (1-280, lanes 1 and 3) and the 3'- end (281-504, lanes 2 and 4) of roX2 with or without ATP in GRNA experiments depicted in Figure 6E are not influenced by differential RNA loading. RNAs were loaded on 1% agarose gels and revealed by SYBR Safe staining. **(D)** Total RNA is extracted from wild-type male larvae (lane 1), *roX1*^{SMC17A} *roX2Δ* male larvae expressing full-length roX2 exon3 (A0B0) (lane 2, UAS construct driven by tubulin-GAL4), wild-type female larvae (lane 3) and *roX1*^{SMC17A} *roX2Δ* male larvae (lane 4), reverse transcribed and checked for roX2 expression by qPCR. Error bars represent +/-SD of three biological replicates. **(E)** Left: Larvae expressing an RFP transgene under the control of a UAS promoter driven either by tubulin-GAL4 (*tub,* left) or *daughterless*-GAL4 (*da*, right) show different levels of expression under a fluorescent microscope. Right: RT-qPCR analysis of total RNA extracted from *roX1*^{SMC17A} *roX2Δ* male larvae expressing full-length roX2 exon3 (A0B0) under a UAS promoter show that the

da-GAL4 driver leads to the accumulation of roX2 RNA that is ~1/3rd of roX2 RNA that accumulates when a tubulin-GAL4 driver is used. **(F)** Top: *tubulin*-GAL4 driven expression of a wild-type (A0B0) roX2 exon3 construct rescues male lethality in *roX1*^{SMC17A} *roX2Δ* mutants (72%). Mutating two helical structures at the 5'-end of the RNA (A1B0) or one important helical structure at the 3'-end (A0B1) did not alter this transgenes ability to mediate dosage compensation (64% and 66% respectively); however, combining those to mutations (A1B1) lead to a poor rescue of male lethality (22%). Error bars represent +/-SEM of at least three biological replicates. Bottom: RT-qPCR analysis of total RNA extracted from the above-mentioned lines show that the stability of the roX2 RNA is comparable in these lines. Error bars represent +/-SD of three biological replicates. **(G)** Top: *daughterless*-GAL4 driven expression of a wild-type roX2 exon3 construct (A0B0) rescues male lethality in *roX1*^{SMC17A} *roX2Δ* mutants similar to *tubulin*-GAL4 driven expression of the same construct (67%). Unlike *tubulin*-GAL4 driven expression though, *daughterless*-GAL4 driven expression of A1B0 and A0B1 mutants lead to a partial loss of male viability upon expression of these constructs in *roX1*^{SMC17A} *roX2Δ* mutant males (43% and 29% respectively) compared to the wild-type construct. Moreover, the combined mutation (A1B1) now leads to a much more severe male-lethality phenotype (1%). Error bars represent +/-SEM of at least three biological replicates. Bottom: RT-qPCR analysis of total RNA extracted from the above-mentioned lines show that the stability of the roX2 RNA is comparable in these lines. (D-G) RNA expression was normalized against phospho fructokinase (PFK). Relative expression is shown in arbitrary units (a.u.). Related to Figure 7.

Supplemental Experimental Procedures

Polytene staining and chromatin immunoprecipitation

Polytene chomosomes from 3rd instar male larvae are squashed and stained as described in (Johansen et al., 2009). Chromatin immunoprecipitation is carried out as described in (Lam et al., 2012). Polyclonal antibodies raised against MLE and MSL1 in rats prepared in-house are used for these experiments (Mendjan et al., 2006). H4K16Ac antibody was purchased from Santa Cruz.

Analysis of ChIP seq data

Reads from the MLE ChIP seq experiment were mapped to the *Drosophila melanogaster* genome using Bowtie (Langmead et al., 2009). To determine the regions significantly bound, the method described in (Conrad et al., 2012) was used. The genome was divided in 25 base pair-wide bins and the number of reads that mapped to each bin was calculated, for both the IP and input. Using DESeq, the relative size factors of IP and input were estimated and the corrected log2 fold-change between them was calculated. The resulting values were smoothed using a 400bp sliding window. By mirroring the left-hand side of the density distribution of the smoothed values, a null distribution was created. Finally, a FDR-adjusted p-value cut-off of 0.05 was used to determine which bins were significantly bound. Genes that had a significantly-bound genes were considered bound by MLE.

MLE tandem-affinity purification

Full-length MLE was tagged at its C-terminus with an HA and a FLAG tag. This construct is cloned into pCaSpER 4 vector under a tubulin promoter and transgenic flies were created by P-element mediated transformation. Insertions on the 3rd chromosome are tested for their ability to rescue male-specific lethality in mle^1 mutant background. Flies with the genotype mle^1; *tub*-MLE-HA-FLAG were expanded, nuclear extracts were prepared from 0-12hrs embryos and MLE is purified as described (Mendjan et al., 2006).

Immunoprecipitation of MSL1

Nuclei from approximately $10x10^6$ S2 cells are prepared by incubating these cells in a hypotonic lysis buffer (HLB: 10mM HEPES-KOH, 10mM KCl, 1,5 mM $MgCl_2$, Protease Inhibitors) for 15 minutes on ice, then vortexing them for 30 seconds after adding Igepal CA 630 detergent to 1%. Nuclei are pelleted by centrifugation, washed once with HLB, re-suspended in KTM-HG (20mM HEPES pH 7.6, 140mM KCl, 2mM $MgCl_2$, 0.2% Tween-20, 1x Complete Protease Inhibitors (Roche)) buffer and sonicated mildly with a Branson sonifier (Output: 1, duty cycle: 40, 20 pulses). The lysate is cleared by centrifugation, after which MSL1 is immunoprecipitated with rabbit polyclonal anti-sera. Immune complexes are collected with Protein A beads (Dynal). After extensive washes with KTM-HG, the samples are either treated with 0.1mg/mL RNase A for 30 minutes at 4˚C or with buffer without any RNAse A. The beads are once again washed extensively with KTM-HG and immunoprecipitated proteins are eluted with 1X LDS buffer, separated by SDS-PAGE and revealed by immunoblotting.

RNAse sensitivity assay

Nuclei from S2 cells are prepared as described above and re-suspended in 25mM HEPES-KOH, 140mM NaCl, 10mM KCl, 1,5mM $MgCl_2$, 0.1% TritonX, 0.2mM EDTA, 25% Glycerol, 1x Complete Protease Inhibitors (Roche). The nuclei split into two, to one half RNaseA is added to 1mg/mL final concentration, only buffer is added to the other half and samples are incubated at 4˚C for 30 minutes. Samples are centrifuged at full-speed for 15 minutes at 4˚C. The supernatant is save as "nucleoplasm" and the pellet as "chromatin fraction". These fractions are made to 1X LDS, proteins are subsequently separated by SDS-PAGE and revealed by immunoblotting.

iCLIP

The rational for choosing iCLIP is that it promises a complete picture of RNA binding through its 5'-tagging strategy via cDNA cyclization instead of RNA ligation. We used Clone8 cells and antibodies against MLE (rat1) and MSL2 (d300, Santa Cruz). One 150mm dish of ~80% confluent cells is used per immunoprecipitation; 6µL from each antibody and 100µL slurry of Protein G (for

MLE) or protein A (MSL2) Dynal beads (Invitrogen). We have isolated nuclei, and used nuclear extracts in all experiments. The low-RNaseI (Ambion) concentration used for library-preparation was 0.5U/mL. Biological triplicates were tagged with different barcodes and mixed together after reverse-transcription.

Reads were separated according to their sample barcodes using sabre (http://github.com/najoshi/sabre). Any sequenced adapters were removed using cutadapt (Martin, 2011). Reads were then mapped to the Drosophila melanogaster genome using bowtie2 (Langmead and Salzberg, 2012). The resulting alignments were post-processed keeping only paired-end reads mapping uniquely to the genome and allowing for up to two mismatches. Random barcodes and coordinates of both ends were used to determine the number of binding events at each cross-linked nucleotide. Errors introduced into the random barcodes during library preparation or sequencing can cause spurious cross-linking events (see Figure S2B-D). In order to compensate for this effect, all cross-linking events associated with fewer reads than 10% of the maximum number of associated reads among the events having the same end coordinates were removed.

Significance of the remaining cross-linked nucleotides was determined in a similar way to (König et al., 2010) and done independently for each replicate. MSL2 replicate 3 was excluded from the remaining analyses due to the very low number of reads (see Figure S2A). Due to the good agreement between replicate profiles for roX1 and roX2 we combined the cross-linking events from the remaining replicates (see Figure S3A-D). All scripts were done using perl, python and fastqpl.

RNA SHAPE analysis

SHAPE is a chemical technique for probing RNA structure, which resolves unpaired RNA bases of a target RNA. When the folded target RNA is treated with an electrophilic SHAPE reagent (here, 2-methylnicotinic acid imidazolide, NAI) the 2'-OH of some bases will react with the reagent. Due to the enhanced nucleophilicity of the 2'-OH of flexible bases, unpaired bases react with NAI more readily than paired, constrained bases. This reaction results in 2'-O-acylation of

unpaired RNA bases, which block elongation of cDNAs by subsequent reverse transcription. Thus, reverse transcription with a radio-labelled reverse primer followed by resolution of "primer stops" by polyacrylamide gel electrophoresis (PAGE) allow the identification of unstructured bases on the target RNA. For RNAs longer than ~100bp, such as the roX RNAs (roX1; 3.7kb and roX2; 0.6kb), multiple reverse primers must be used to analyze the RNA structure piecemeal.
For each SHAPE reaction, 2pmol of RNA in 6μL 0.5XTE buffer was refolded by heating to 95ºC for 2 min, cooling on ice, adding 3uL 3.3X folding buffer, and incubating at 28ºC for 20 min. The folded RNA was then treated with either NAI (1μL, 500mM in DMSO) or neat DMSO alone for the (+) and (–) NAI reactions, respectively, and incubated at 28ºC for 30min. Treated RNA was recovered by PCIA-EP and re-suspended in 10uL 0.5XTE.

Detecting modification sites by primer extension

Radiolabeled reverse primer was added to RNA from (+) or (–) NAI reactions, and the RT reaction was heated to 95ºC for 2 min and slowly cooled to 4ºC at 10ºC/min. Primer extension reactions were setup with reaction mix (6μL; 250mM KCl; 167mM Tris-HCl [pH8.3]; 10mM $MgCl_2$; 1.67mM each dATP, dCTP, dGTP, and dTTP; 16.7mM DTT) and pre-incubated at 52ºC for 1 min before adding Superscript III (1μL, 200 units; Invitrogen). Sequencing reactions were carried out in parallel with dideoxynucleotides (ddATP and ddTTP). Primer extension continued for 10 min at 52ºC. The reaction was stopped and RNA hydrolyzed by adding NaOH (1μL, 4M) and heating to 95ºC for 5min. Gel Loading Buffer II (10μL; Invitrogen) was added to each reaction, and run on denaturing 8% polyacrylamide gel electrophoresis with 7M Urea. The resulting gel was dried (Labconco Gel Dryer), exposed to a storage phosphor screen (Molecular Dynamics) for 16 hrs, and scanned (GE Typhoon Trio). Band intensities were measured using Semi-Automated Footprinting Analysis (SAFA, simtk.org). To calculate SHAPE reactivity, the unmodified RNA bands were subtracted from the modified RNA bands, then normalized such that the average of the top 10% of reactivities is 1.

PARS analysis

PARS reactions, library construction, sequencing, and data processing performed as in (Kertesz et al., 2010). The PARS score of each base is calculated as LOG2[(V1 reads + 1)/(S1 reads + 1)] and the data is filtered to include the top 20% covered bases so as to eliminate noise from poor sequencing coverage.

GRNA Chromatography

GRNA protocol is adapted from (Czaplinski et al., 2005) and (Duncan et al., 2006).

Cloning and synthesis of boxB tagged RNAs

All RNAs used in GRNA chromatography were made by *in vitro* transcription using the Ribomax T7 kit from Promega. The run-off transcripts were purified using Megaclear columns (Ambion). The templates were all cloned into pBlueScript KS (pBS) and linearized with Asp718 or XhoI after which the 3'-ends were filled in with Klenow (NEB) and purified by phenol/chloroform extraction.

The sequence of the boxB tag used in this study is as follows:

GGGCCCUGAAGAAGGGCCC

Two tandem copies of boxB RNA are cloned into pBS by annealing the following oligos and ligating them into SacI-NotI digested pBS:

Up:CGGGCCCTGAAGAAGGGCCCAAGACGTCAAGGGCCCTGAAGAAGGGCCCAGATCT TATAAGC

Down:GGCCGCTTATAAGATCTGGGCCCTTCTTCAGGGCCCTTGACGTCTTGGGCCCT TCTTCAGGGCCCGAGCT creating pBS155.

GFP RNA is generated by amplifying pEGFP-C2 (Clontech) with the following primers:

L: ATATctgcagcctgaagttcatctgcacca

R: ATATctcgagtgttctgctggtagtggtcg

This was followed by cloning the 450bp product into pBS155 by PstI-XhoI digestion and ligation.

roX2 exon-3 (1-280) is generated by amplifying *Drosophila* gDNA with:

L: ATACTGCAGTAGCTCGGATGGCCATCG

R: CTCGAGATATCTATTGCATATTGTATATTGTATATTG
This was followed by cloning the product into pBS155 by PstI-XhoI.

roX2 exon-3 (281-504) is generated by amplifying *Drosophila* gDNA with
L: ctgcaGATATCAATACAATACAAGACAAAAAAATG
R: ACTCGAGTATTATTTGGCAATTGTTAAG
This was followed by cloning the product into pBS155 by PstI-XhoI.

roX2 exon-3 (1-504) was created by digesting pBS155_roX2exon3_281-504 with EcoRV and XhoI and cloning this fragment into EcoRV-XhoI digested pBS155_roX2exon3_1-280.
The stem-mutants were created by *de novo* gene synthesis (Eurofins-MWG) and cloned into pBS155_roX2exon3_1-504 via PstI-EcoRV digestion and ligation.
Following are the wild-type sequences and the mutant forms (underlined) used in GRNA chromatography:

R2H1 wild-type:
(…)GCTTTAGAGATCGTTTCGAATCACATTGATAATCGTTCGAAACGTTCTCCGAAGC(…)
R2H1 mutant:
(…)CGAATAGAGATGCAAAGCTATCACATTGATAATCGTTCGAAACGTTCTCCGAAGC(…)
R2H2 wild-type:
(…)GATTTCCGCATAGTCGAAAATGTTTAAGTTGAATTGTCTTACGGACAGTGAGATGAGTACGACTATTTGGAAATC(…)
R2H2 mutant:
(…)CTAAAGGGCATTCAGGAAAATGTTTAAGTTGAATTGTCTTACGGACAGTGAGATGAGTACGACTATTTGGAAATC(…)
P3 wild-type:
(…)TTGTTTTCATGGTTGACGCGCTTGTCAAGCTACAAAACAA(…)
P3 mutant:
(…)TTATCTTCATCCGAGAGCCGCTTGTCAAGCTACAAAACAA(…)
R2H1-R2H2 mutant is the combination of P1 mutant and P2 mutant.

roX1 constructs for GRNA chromatography:

D1:

L: ATATctgcagGAGATTCTTCGCCTGAGCTG

R: ATATctcgagGTGCGGTCTGAACTTTTTCC

U1:

L: ATATctgcagAGACCGCACTCACGAATACC

R:ATATctcgagTGCAGTGGCAGTTTCTTCTG

D2:

L: ATATctgcagTGGAAAACGTTGAGTAGGGG

R: ATATctcgagGGCTCCAAGTTTCGTCTCTG

U2:

L: ATATggatccCAGAGACGAAACTTGGAGCC

R: ATATctcgagAAGTCAAGGAAGGGGACTGG

D3 (1-450):

L: ATATctgcagTTTTGTCCCACCCGAATAAC

R: ATATctcgagATTCGCTTTATTGTGCTCCG

D3 (1-188):

L: ATATctgcagTTTTGTCCCACCCGAATAAC

R: ATATctcgagCTTCTTGAACCGTAATGAATGCATAG

D3 (230-450):

L: ATATctgcagCACATTTACTAACAAATAAAAACTTGCT

R: ATATctcgagATTCGCTTTATTGTGCTCCG

D3 (1-118):

L: ATATctgcagTTTTGTCCCACCCGAATAAC

R: ATATctcgagTTTAAATGTGATTCCCATTTCG

D3 (119-450):
L: ATATctgcagATTTTGAACTGCGTAAAACGAA
R: ATATctcgagATTCGCTTTATTGTGCTCCG

cDNA prepared from male flies is amplified by PCR with the primers indicated above, digested with PstI-XhoI and ligated into p155 digested with PstI-XhoI , with the exception of U2, which is digested with BamHI and XhoI and ligated to p155 digested with BamHI and XhoI. The resulting plasmids are sequence verified and used in IVT after linearization with Asp718.

Expression and purification of GST•λ•6His

The plasmid used for the expression of GST•λ•6His was a kind gift from Matthias Hentze. GST•λ•6His requires the co-expression of rare codon expressing bacteria and BL21(DE3) CodonPlus was used for this purpose. GST•λ•6His was purified to near homogeneity using single-step IMAC (Ni-NTA, Qiagen).

GRNA Chromatography Protocol

26µg GST•λ•6His is incubated with 60µL slurry of Magnetic GST beads (Thermo) for 1hr at 4˚C in binding buffer (BB100, 50mM Tris•Cl pH 7.6, 100mM KCl, 1.5mM $MgCl_2$, 0.1% Igepal CA-630 (Sigma), 10% Glycerol, 0.1mg/mL tRNA [Roche], 0.01mg/mL Heparin, 1x Protease inhibitor coctail [Roche]) and washed several times with BB. Then 20pmol of RNA is incubated with the GST•λ•6His bound beads in BB+40u/mL RNasin (Promega) for 12-16hrs. The beads are washed twice with BB and are then incubated with 250-500µg of embryonic nuclear extract (KCl method(Santoso and Kadonaga, 2006) final [KCl]: 150mM) in 300µL BB+40u/mL Rnasin for 45 minutes at 18˚C. ATP is added to 3mM when indicated. The beads are washed with BB100 extensively. Before elution with RNAse A, beads are split into two and RNA is extracted using RNeasy MinElute kit (Qiagen) and visualized with SYBR gold after agarose gel electrophoresis. Bound proteins were eluted with 30µL BB with 50mM without tRNA or Heparin and with 1µg RNaseA (Fermentas) at 30˚C for 30 minutes. The eluate was analyzed by immunoblotting.

GRNA Chromatography using S2 cells

MLE^{wt}, MLE^{GET} and MLE^{KHR} are cloned into pIBU2 vector together with a C-terminal HBH tag (Tagwerker et al., 2006). $20x10^6$ S2 cells were transfected with 4µg of each construct using Effectene reagent. 24hrs later, the cells are collected by centrifugation, nuclei are isolated as described above and are re-suspended BB100. The salt is increased to 420mM KCl to extract nuclear proteins. Before using the extracts for GRNA chromatography, the salt concentrations is brought back to 105mM KCl by slow addition of BB10.

Electrophoretic Mobility Shift Assay (EMSA)

EMSAs were performed in the following buffer: 25mM Tris.Cl pH 7.5, 75mM NaCl, 1.5mM $MgCl_2$, 1mM DTT 0.1mg/mL BSA (NEB), 0.1mg/mL tRNA (E. coli, Roche), 0.05% Igepal CA 630. RNA-protein complexes were separated in 4% native Tris-Glycine PAA gels and imaged using Typhoon FLA7000 (GE Healthcare).

The proteins (MLE^{1-254}, $MLE^{1-254(KHRmutant)}$, GST-dsRBD1 and GST-dsRBD2) were purified using IMAC (TALON, Clontech) and gel-filtration.

The following primer were used to generate templates for *in vitro* transcription reactions:

For R2H1-R2H2 probes in Figure 6C, Figure S6B,D,E and F):

L: GAATTAATACGACTCACTATAGGGTCGAAAGGGTAAATTGGTGTTAC

R: CGTCAACCATGAAAACAATTCG

Templates for PCR were chosen from the mutants cloned into p155 described above.

For the 5'-end of roX2 exon-3 (1-265, Figure S6C and F):

L: GAATTAATACGACTCACTATAGGGTCGAAAGGGTAAATTGGTGTTAC

R: TATTGCATATTGTATATTG

For 3'-end of roX2 exon-3 (281-504, Figure S6C and F):

L: GAATTAATACGACTCACTATAGGGATATCAATACAATACAAGAC

R: CAATTGTTAAGTTTCGTATAAC

RNA probes were prepared by IVT and tagged by activating their 5'-ends of RNA with PNK/γ-thio-ATP and labeling them with maleimide-Alexa647.

RNAi in S2 cells, total RNA isolation, reverse transcription

RNAi is performed by soaking the cells with dsRNA prepared by *in vitro* transcription. 20μg of dsRNA was used per 1 million cells in 6-well plates. Cells are washed with PBS and lysed with 1XLDS for immunoblotting or with RLT for RNA extraction. The following primers are used to generated templates for IVT:

GFP	L: TGAAGTTCATCTGCACCACC
	R: AGTTCACCTTGATGCCGTTC
MLE	L:CCACGTGGCAATGATTGTAG
	R: GCAATTCACCGAGGTTTTGT

The T7 promoter sequence (ATATAATACGACTCACTATAGGG) precedes each primer.

roX2 cloning and RNA transcription for SHAPE and PARS analysis

Total RNA from Clone 8 (*Drosophila* Genome Resource Center) cells was extracted using TRIZol reagent (Invitrogen), and treated with TURBO DNase (Ambio). roX2 cDNA was reverse transcribed from purified total RNA using roX2-Rprimer (5'-TTATTTGGCAATTGTTAAGTTTCGTATAAC) and Superscript III First Strand Synthesis System (Invitrogen). roX2 cDNA was PCR amplified with rox2-Rprimer and roX2-Fprimer (5'-TGTTGCGGCATTCGCGGCCTGGTCA) using Phusion High-Fidelity PCR Master Mix (New England Biolabs). Resulting roX2 cDNA was cloned into pCRII Blunt TOPO vector using Zero Blunt TOPO PCR cloning kit (Invitrogen) and transformed into One Shot TOP10 competent cells (Invitrogen). Amplified plasmids from selected colonies were sequenced to confirm correct roX2 insert. The *in vitro* transcription DNA template was

constructed by PCR amplifying the roX2 sequence with T7-roX2_Fprimer (5'-TAATACGACTCACTATAGG TGTTGCGGCATTCGCGGCCTGGTCA) and Adapter-roX2_Rprimer (5'-GAACCGGACCGAAGCCCGATTTG TTATTTGGCAATTGTTAAGTTTCGTATAAC) and the PCR product was run on agarose gel electrophoresis and extracted with QIAquick Gel Extraction Kit (QIAGEN). roX2 RNA was transcribed using MEGAscript T7 *in vitro* transcription kit (Invitrogen), DNase-treated, and purified by phenol-chlorofom-isoamyl alcohol extraction and ethanol precipitation (PCIA-EP).

roX1 cloning and RNA transcription for SHAPE analysis

The roX1 gene was amplified from Clone 8 genomic DNA using roX1-Fprimer (5'-TTAATGCGTAGTCACCGAAGAAAAGTG) and roX1-Rprimer (5'-CTTTGTGAATCGGCTCAGGCG) and cloned into pCRII vector as above. The *in vitro* transcription DNA template was constructed by PCR amplifying the roX1 sequence with T7-roX1-Fprimer (5'-TAATACGACTCACTATAGG TTAATGCGTAGTCACCGAAGAAAAGTG) and Adapter-roX2-Rprimer (5'-GAACCGGACCGAAGCCCGATTTG CTTTGTGAATCGGCTCAGGCG) and purified and transcribed as above.

HITS-CLIP

HITS-CLIP was performed as described in (Chi et al., 2009) with the following modifications: Nuclear extracts prepared from Drosophila S2 cells were used for immunoprecipitations. After high-salt washes, the 3'-ends of bound RNAs were de-phosphorylated first with PNK in MES-PNK buffer (25mM MES @ pH 6.0, 50mM NaCl, 10mM $MgCl_2$, 0.1% Tween20, 5mM DTT, NO ATP, 1U/μL PNK [NEB]) by incubating the beads at 37°C for 10 minutes and then with CIP (NEB) before ligation of the 3'-RNA tag. During our analysis, we have encountered an interesting phenomenon that has not been described previously. Some of the CLIP-tags that mapped to roX2 RNA had gaps in the middle of the sequence, ranging from a few base pairs up to eight base pairs or more. Curiously, most of these gaps correspond to the loop region of R2H1, suggesting that MLE interaction protected the stems from degradation, and that an intra-molecular ligation event sealed the loop cleaved by RNaseI. A recent study has exploited a

similar phenomenon where infrequent inter-molecular ligation events that lead to hybrid RNA molecules were used to elucidate RNA-RNA interactions *in vivo* (Kudla et al., 2011).

Fly culture and genetics

Flies (*Drosophila melanogaster*) were reared on standard fly medium at 25°C and 70% relative humidity and 12 hrs dark/12 hrs light cycle. All transgenic lines carrying wild type or mutant versions of exon-3 of roX2 were generated through phiC31 integrase-mediated germ-line transformation as previously described (Groth et al., 2004) to avoid the influence of position effects on gene expression and to facilitate direct comparison upon phenotypic analysis. Plasmid DNA was injected into *y^1 M{vas-int.Dm}ZH-2A w*; PBac{y^+-attP-3B}VK00033* embryos (Bloomington stock #24871), that carried an *attP* docking site at position 65B2 on chromosome arm 3L (Venken et al., 2006) and a Drosophila codon-optimized ΦC31 integrase driven in the germline by the *vasa* promoter (Bischof et al., 2007). PCR confirmation of proper integration into the docking site was performed on DNA isolated from single flies using the so called squishing method (Gloor et al., 1993). PCR primers and conditions were as previously described (Venken et al., 2006).

The following stocks were obtained from the Bloomington stock centre or were kindly donated: y^1 w^1 N^{spl-1}/Dp(1;Y)B^S;mle^1/SM1(Bloomington stock#4235) *y^1 w*; P{tubP-GAL4}LL7/TM3, Sb^1* (Bloomington stock #5138), *w^{1118};P{da-GAL4.w-}3* (Bloomington stock #8641), *$roX1^{SMC17A}$, $roX2^{\Delta}$*; *CyO, hsp83-roX1* (Menon and Meller, 2012). *roX* mutant alleles have been previously described *$roX1^{SMC17A}$* (Deng et al., 2005) and r*$oX2^{\Delta}$* (Menon and Meller, 2012).

All lines used in this study were generated by standard genetic crosses from the above listed fly stocks.

Analysis of male –specific lethality rescue

To determine the male viability frequency upon ectopic expression of UAS-roX2*, *$roX1^{SMC17A}$, $roX2^{\Delta}$*; *CyO, hsp83-roX1*; *tubGal4/TM6BTb* virgin females were crossed to A0B0, A1B0, A2B0, A3B0, A0B1, A0B2, A0B3, A0B4, A0B5, A1B1, A1B4, A2B4 or A3B4 (mutations are described below) males. Male and female adult flies from

at least three independent crosses were counted daily for a period of 10 days from the start of eclosion. The total number of males was divided by the total number of females that eclosed during the 10-day period, used as an internal control for 100% viability.
Females showed similar viability and rate of eclosion for all roX2 transgenic lines.

All the roX2 exon-3 constructs are of the same length and sequence with the exception of the mutations indicated below:

A0: wt roX2 exon-3, 1-280
A1: R2H1mut R2H2mut
Described above.
A2: R2H3mut P3mut

wild-type:
(…)GAATTGTCTTACGGA(…)ATTGTTTTCATGGTTGACGCGC(…)
mutant:
(…)GAAAACAGAATGGGA(…)ATTATCTTCATCCGAGAGCCGC(…)

A3: R2H1mut R2H2mut R2H3mut P3mut
Combination of A1 and A2 mutations.
B0: wt roX2 exon-3, 281-504.
B1: R2H5mut (5'-stem)

wild-type:
(…)TAAAAGACGTGTAAAATGTTGCAAATTAAG (…)
mutant:
(…)TAATTCACGGCATAAAGCAAGCAAATTAAG(…)

B2: R2H5mut (3'-stem)
wild-type:
(…)GGTTTGTAATATGTCGCGAAAAC (…)

mutant:

(…)GGTAACGTTTTACGCGCCTTAAC (…)

B3: R2H6mut

wild-type:

(…)TGATTGTAAAATGTAAAGAAAAC (…)

mutant:

(…)TGAAATGTTATACGAAACTTAAC (…)

B4: R2H5mut (3'-stem) R2H6mut

Combination of B2 and B3 mutations.

B5: R2H4mut R2H5mut (3'-stem) R2H6mut

Combination of B2, B3 and the following mutation:

wild-type:

(…)TGGTTGTCAAGTAATATCAA (…)

mutant:

(…)TGGAACGCAACATTGTACAA (…)

Mutations are generated by *de novo* gene synthesis. All constructs were cloned into p155 as described above by combining A and B fragments using appropriate restriction enzymes (PstI-EcoRV-XhoI) and then sub-cloned into pUASattB using BglII-XhoI.

Analysis of roX2 RNA stability in transgenic males

Total RNA was isolated from wandering third instar larvae using Trizol followed by ethanol precipitation. Genomic DNA is removed using TURBO DNaseI. Resulting RNA is reverse transcribed using SuperScriptIII according to manufacturer's protocol and analysed by quantitative PCR using the following primer pairs:

roX2:

L: GCCATCGAAAGGGTAAATTG

R: CTTGCTTGATTTTGCTTCGG

Phosphofructokinase (pfk):

L: CTGAGGGCAAGTTCAAGGAG
R: AAGCCACCAATGATCAGGAG

roX2 levels were normalized to pfk levels in biological and technical replicates. At least two biological replicates were used for all the tubulin-GAL4 driven constructs.

Supplemental References

Bischof, J., Maeda, R.K., Hediger, M., Karch, F., and Basler, K. (2007). An optimized transgenesis system for Drosophila using germ-line-specific phiC31 integrases. Proc Natl Acad Sci U S A *104*, 3312-3317.

Chi, S.W., Zang, J.B., Mele, A., and Darnell, R.B. (2009). Argonaute HITS-CLIP decodes microRNA-mRNA interaction maps. Nature *460*, 479-486.

Conrad, T., Cavalli, F.M., Vaquerizas, J.M., Luscombe, N.M., and Akhtar, A. (2012). Drosophila dosage compensation involves enhanced Pol II recruitment to male X-linked promoters. Science *337*, 742-746.

Czaplinski, K., Kocher, T., Schelder, M., Segref, A., Wilm, M., and Mattaj, I.W. (2005). Identification of 40LoVe, a Xenopus hnRNP D family protein involved in localizing a TGF-beta-related mRNA during oogenesis. Dev Cell *8*, 505-515.

Deng, X., Rattner, B.P., Souter, S., and Meller, V.H. (2005). The severity of roX1 mutations is predicted by MSL localization on the X chromosome. Mech Dev *122*, 1094-1105.

Duncan, K., Grskovic, M., Strein, C., Beckmann, K., Niggeweg, R., Abaza, I., Gebauer, F., Wilm, M., and Hentze, M.W. (2006). Sex-lethal imparts a sex-specific function to UNR by recruiting it to the msl-2 mRNA 3' UTR: translational repression for dosage compensation. Genes Dev *20*, 368-379.

Gloor, G.B., Preston, C.R., Johnson-Schlitz, D.M., Nassif, N.A., Phillis, R.W., Benz, W.K., Robertson, H.M., and Engels, W.R. (1993). Type I repressors of P element mobility. Genetics *135*, 81-95.

Groth, A.C., Fish, M., Nusse, R., and Calos, M.P. (2004). Construction of transgenic Drosophila by using the site-specific integrase from phage phiC31. Genetics *166*, 1775-1782.

Johansen, K.M., Cai, W., Deng, H., Bao, X., Zhang, W., Girton, J., and Johansen, J. (2009). Polytene chromosome squash methods for studying transcription and epigenetic chromatin modification in Drosophila using antibodies. Methods *48*, 387-397.

Kelley, R.L., Lee, O.K., and Shim, Y.K. (2008). Transcription rate of noncoding roX1 RNA controls local spreading of the Drosophila MSL chromatin remodeling complex. Mech Dev *125*, 1009-1019.

Kertesz, M., Wan, Y., Mazor, E., Rinn, J.L., Nutter, R.C., Chang, H.Y., and Segal, E. (2010). Genome-wide measurement of RNA secondary structure in yeast. Nature *467*, 103-107.

Kudla, G., Granneman, S., Hahn, D., Beggs, J.D., and Tollervey, D. (2011). Cross-linking, ligation, and sequencing of hybrids reveals RNA-RNA interactions in yeast. Proc Natl Acad Sci U S A *108*, 10010-10015.

Lam, K.C., Muhlpfordt, F., Vaquerizas, J.M., Raja, S.J., Holz, H., Luscombe, N.M., Manke, T., and Akhtar, A. (2012). The NSL complex regulates housekeeping genes in Drosophila. PLoS Genet *8*, e1002736.

Langmead, B., and Salzberg, S.L. (2012). Fast gapped-read alignment with Bowtie 2. Nat Methods *9*, 357-359.

Langmead, B., Trapnell, C., Pop, M., and Salzberg, S.L. (2009). Ultrafast and memory-efficient alignment of short DNA sequences to the human genome. Genome Biol *10*, R25.

Martin, M. (2011). Cutadapt removes adapter sequences from high-throughput sequencing reads, Vol 17.

Mendjan, S., Taipale, M., Kind, J., Holz, H., Gebhardt, P., Schelder, M., Vermeulen, M., Buscaino, A., Duncan, K., Mueller, J.*, et al.* (2006). Nuclear pore components are involved in the transcriptional regulation of dosage compensation in Drosophila. Mol Cell *21*, 811-823.
Menon, D.U., and Meller, V.H. (2012). A role for siRNA in X-chromosome dosage compensation in Drosophila melanogaster. Genetics *191*, 1023-1028.
Santoso, B., and Kadonaga, J.T. (2006). Reconstitution of chromatin transcription with purified components reveals a chromatin-specific repressive activity of p300. Nat Struct Mol Biol *13*, 131-139.
Stuckenholz, C., Meller, V.H., and Kuroda, M.I. (2003). Functional redundancy within roX1, a noncoding RNA involved in dosage compensation in Drosophila melanogaster. Genetics *164*, 1003-1014.
Tagwerker, C., Flick, K., Cui, M., Guerrero, C., Dou, Y., Auer, B., Baldi, P., Huang, L., and Kaiser, P. (2006). A tandem affinity tag for two-step purification under fully denaturing conditions: application in ubiquitin profiling and protein complex identification combined with in vivocross-linking. Mol Cell Proteomics *5*, 737-748.
Venken, K.J., He, Y., Hoskins, R.A., and Bellen, H.J. (2006). P[acman]: a BAC transgenic platform for targeted insertion of large DNA fragments in D. melanogaster. Science *314*, 1747-1751.